

First few overtones probe the event horizon geometry

R. A. Konoplya ^{1,*} and A. Zhidenko ^{2,†}

¹*Research Centre for Theoretical Physics and Astrophysics, Institute of Physics,
Silesian University in Opava, Bezručovo náměstí 13, CZ-74601 Opava, Czech Republic*

²*Centro de Matemática, Computação e Cognição (CMCC), Universidade Federal do ABC (UFABC),
Rua Abolição, CEP: 09210-180, Santo André, SP, Brazil*

It is broadly believed that quasinormal modes cannot tell the black-hole near-horizon geometry, because usually the low-lying modes are determined by the scattering of perturbations around the peak of the effective potential. Using the general parametrization of the black-hole spacetimes respecting the generic post-Newtonian asymptotic, we will show that tiny modifications of the Schwarzschild/Kerr geometry in a relatively small region near the event horizon lead to almost the same Schwarzschild/Kerr fundamental mode, but totally different first few overtones. Having in mind that the first several overtones affect the quasinormal ringing at its early and intermediate stage [M. Giesler, M. Isi, M. Scheel, and S. Teukolsky, *Phys. Rev. X* 9, 041060 (2019)], we argue that the near-horizon geometry could in principle be studied via the first few overtones of the quasinormal spectrum, which is important because corrections to the Einstein theory must modify precisely the near-horizon geometry, keeping the known weak field regime.

I. INTRODUCTION

The proper oscillation frequencies of black holes, quasinormal modes (QNMs) [1–4], govern the decay of perturbations of black holes and the fundamental mode, which has the smallest decay rate, dominates at late times of the black holes’ ringdown. Therefore, within the astrophysical context the fundamental mode was the one mostly studied in the literature. Despite the quasinormal frequencies do not depend on the way of perturbations, but only on the parameters of black holes, it was shown that the ringdown profile may not probe the geometry of the event horizon [5], so that even qualitatively different compact objects, such as wormholes [5–7] can mimic the black hole ringdown. This happens because the main part of the scattering from the effective potential surrounding the black hole occurs near the peak of the potential barrier and this region determines the dominant QNMs. Deformations of the geometry only near the event horizon do not alter those dominant frequencies. If the near-horizon deformation is such that an additional peak appears near the surface of the compact body, then at very late times the decay of gravitational waves are slightly modified by echoes [5], while the fundamental mode remains again essentially unaffected. Actually the same logic is applicable to other astrophysically relevant phenomena, such as particles’ motion, lensing etc., so that in addition to the weak and elusive echoes [8], only the Hawking radiation tells the properties of the event horizon [6].

Although it is believed that the major contribution to the signal is owing to the fundamental mode, recently it has been shown [9] (and later studied in [10–12]) that the first several overtones must be taken into account in order to model the ringdown phase, obtained within the accurate numerical relativity simulations at the beginning of

the quasinormal ringing and not only at the last stage. This finding indicated also that the actual quasinormal ringing starts earlier than expected. In [13] it was shown that an independent measurement of the quasinormal frequency of the first overtone leads to agreement with the no-hair hypothesis at the 20% level. When the detector sensitivity and the observable population of black-hole mergers increase, one can expect that overtones will provide more efficient tests of the strong gravity regime [13].

Once the overtones are taken into account, the modelling and linear profile of the ringdown are in full concordance and allow to extract angular mass and momentum of the black hole. The posterior analysis of LIGO’s observational data from the GW150914 gravitational-wave signal [14] provides evidence for the presence of the first overtone rather than noise [15, 16]. Therefore, detection of the higher overtones is expected in the near future as the signal-to-noise ratio improves with the next-generation gravitational-wave detectors, such as the Einstein Telescope [17], Cosmic Explorer [18], and the space-based interferometer LISA [19]. Although the current sensitivity of the LIGO/VIRGO detectors does not yet allow for the unambiguous detection of the overtones in the gravitational-wave signals [20, 21] and the non-linear corrections must be taken into account when analyzing the higher-overtones contributions [22–24], there are indications that the overtones are significantly excited in some events and can be detected by LISA at the early ringdown phase [25].

Having in mind the above motivation, we will consider the general parametrized spherically and axially symmetric black holes, respecting the experimentally allowed post-Newtonian behavior [26]. There are two sets of parameters: experimentally constrained ones, determining the weak field regime at a distance from the black hole and the ones fixed by the near-horizon strong gravity region. We show that deformations of the near-horizon parameters induce outburst of overtones, while the fundamental mode changes insignificantly. This observation

* roman.konoplya@gmail.com

† olexandr.zhydenko@ufabc.edu.br

is important, because essentially non-Einsteinian behavior is expected exactly near the event horizon, either due to quantum corrections or alternative theories of gravity (see e.g., [27]), including the brane-world models. Since the fundamental mode should not be affected strongly by such near-horizon corrections, one can expect that the dominant nonlinear effects due to this mode [22–24] do not lead to the significant deviations from the Kerr ringdown profile as well.

This way, the first few overtones, which potentially could be extracted from the beginning of the time-domain profile of quasinormal ringing could probe the near-horizon geometry of a black hole and, for example, distinguish a black-hole mimicker. The latter might be more profitable way than echoes, which occur at very late times when the amplitude of the signal is strongly damped.

Here we would like to provide a brief clarification on terminology. When discussing the alterations to the geometry of a black hole relative to its Schwarzschild/Kerr limit, induced by alternative theories or other factors, the term “perturbations” is occasionally employed. In fact, what is typically referred to as “perturbations” in those papers [28–30] is merely the addition of a small function of the radial coordinate to the initial black hole metric, such as the Schwarzschild metric. This function is independent of time. Specifically:

$$g_{\mu\nu}(r, \theta, \phi) \rightarrow g_{\mu\nu}(r, \theta, \phi) + \delta g_{\mu\nu}(r) \quad - \text{deformation.} \quad (1)$$

The perturbation of any given static or stationary black hole spacetime, however, must be time-dependent and is responsible for dynamical degrees of freedom:

$$g_{\mu\nu}(r, \theta, \phi) \rightarrow g_{\mu\nu}(r, \theta, \phi) + \delta g_{\mu\nu}(t, r, \theta, \phi) \quad - \text{perturbation.} \quad (2)$$

The mere smallness of the added term is not sufficient to call it a “perturbation”. This addition does not correspond to any dynamical degree of freedom; rather, it simply modifies the background metric geometry in a static manner. When considering a stationary metric, such as Kerr, as the “non-perturbed background”, the added term remains stationary and time-independent.

Therefore, we find this term misleading as it may be mistaken for perturbations of an already deformed stationary geometry of a black hole. Similarly, the set of perturbations for these deformed non-Schwarzschild/non-Kerr black holes is sometimes referred to as a “quasi-spectrum”, despite it being the typical spectrum of quasinormal modes for a specific black hole geometry. Hence, we opt to refrain from using the terms “perturbations” and “quasi-spectrum”, instead preferring “deformation” and “spectrum of the deformed black hole”, respectively. The same logic applies to the term “(in)stability” of the frequencies. This refers to the fact that the frequencies of the deformed black hole deviate from their Schwarzschild values at an increasing rate while the deformation remains small. Such “(in)stability” can be confused with the concept of dynamical instability caused by small time-dependent perturbations, where certain modes grow

unboundedly over time, leading to a situation where the entire configuration becomes unsustainable.

II. BASIC EQUATIONS

A. The general parametrized black-hole metric

The metric of a spherically symmetric black hole can be written in the following general form,

$$ds^2 = -N^2(r)dt^2 + \frac{B^2(r)}{N^2(r)}dr^2 + r^2(d\theta^2 + \sin^2\theta d\phi^2), \quad (3)$$

where r_0 is the event horizon, so that $N(r_0) = 0$. Following [31], we will use the new dimensionless variable

$$x \equiv 1 - \frac{r_0}{r},$$

so that $x = 0$ corresponds to the event horizon, while $x = 1$ corresponds to spatial infinity. We rewrite the metric function N via the expression $N^2 = xA(x)$, where $A(x) > 0$ for $0 \leq x \leq 1$. Using the new parameters ϵ , a_0 , and b_0 , the functions A and B can be written as

$$\begin{aligned} A(x) &= 1 - \epsilon(1-x) + (a_0 - \epsilon)(1-x)^2 + \tilde{A}(x)(1-x)^3, \\ B(x) &= 1 + b_0(1-x) + \tilde{B}(x)(1-x)^2. \end{aligned} \quad (4)$$

Here the coefficient ϵ measures the deviation of r_0 from the Schwarzschild radius $2M$:

$$\epsilon = \frac{2M - r_0}{r_0}.$$

The coefficients a_0 and b_0 can be considered as combinations of the post-Newtonian (PN) parameters,

$$a_0 = \frac{1}{2}(\beta - \gamma)(1 + \epsilon)^2, \quad b_0 = \frac{1}{2}(\gamma - 1)(1 + \epsilon).$$

Current observational constraints on the PN parameters imply $a_0 \sim b_0 \sim 10^{-4}$, so that we can safely neglect them.

The functions \tilde{A} and \tilde{B} are introduced through infinite continued fraction in order to describe the metric near the horizon (i.e., for $x \simeq 0$),

$$\tilde{A}(x) = \frac{a_1}{1 + \frac{a_2 x}{1 + \frac{a_3 x}{1 + \dots}}}, \quad \tilde{B}(x) = \frac{b_1}{1 + \frac{b_2 x}{1 + \frac{b_3 x}{1 + \dots}}}, \quad (5)$$

where a_1, a_2, \dots and b_1, b_2, \dots are dimensionless constants to be constrained from observations of phenomena which are localized near the event horizon. At the horizon only the first term in each of the continued fractions survives,

$$\tilde{A}(0) = a_1, \quad \tilde{B}(0) = b_1,$$

which implies that near the horizon only the lower-order terms of the expansions are essential. For instance, the

Hawking temperature depends on the coefficients of the lowest order only [32],

$$T_H \equiv \frac{\kappa_g}{2\pi} = \frac{A(0)}{4\pi B(0)} = \frac{1 - 2\epsilon + a_0 + a_1}{4\pi r_0(1 + b_0 + b_1)}. \quad (6)$$

When all the coefficients a_i , b_i and ϵ vanish, we have the Schwarzschild black hole, so that one can consider the above parametrization as a general deformation of the Schwarzschild geometry. Then, we would like to understand which kind of deformations are responsible for the outburst of overtones. For this purpose, following [33], we will distinguish the Schwarzschild-like *nonmoderate* black holes, whose metric functions are close to the Schwarzschild one everywhere except for a relatively small region near the event horizon, in which it is strongly different. The word *relatively* means here that the deformation must decay and be negligibly small near the peak of the potential barrier. It is believed that this kind of black holes can be Schwarzschild mimickers, so that their ringdown profile and shadows are practically indistinguishable from those for the Schwarzschild ones [33, 34]. *Moderate* black holes are characterized by relatively slow change of the metric functions in the near horizon zone.

B. Calculation of the quasinormal modes

After the separation of variables in the general covariant equations for the scalar and electromagnetic perturbations they can be reduced to the Schrödinger-like form (see, e.g., [4]),

$$\frac{\partial^2 \Psi}{\partial t^2} - \frac{\partial^2 \Psi}{\partial r_*^2} + V(r)\Psi = 0, \quad (7)$$

where the ‘‘tortoise coordinate’’ r_* is defined by the relation

$$dr_* = \frac{B(r)dr}{N^2(r)}.$$

The effective potentials for the scalar and electromagnetic fields are

$$V(r) = N^2(r) \frac{\ell(\ell+1)}{r^2} + \frac{1-s}{2r} \frac{d}{dr} \frac{N^4(r)}{B^2(r)},$$

where $\ell = 1, 2, \dots$ are the multipole numbers and $s = 0$ ($s = 1$) corresponds to the scalar (electromagnetic) field, respectively. The effective potential for the electromagnetic field has the form of the positive definite potential barrier, while this is not always so for a scalar field.

Quasinormal modes ω_n are frequencies corresponding to solutions of the master wave equation (7) with the requirement of the purely outgoing waves at infinity and at the event horizon, $\Psi \propto e^{-i\omega t \pm i\omega r_*}$, $r_* \rightarrow \pm\infty$. In order to find QNMs we will use two methods: the time-domain integration and the Frobenius method.

In the time domain, we integrate the wavelike equation (7) in terms of the light-cone variables $u = t - r_*$ and $v = t + r_*$, using the discretization scheme of [35] and, further, extracting QNMs with the Prony method [36].

In the frequency domain, after separating the time and radial coordinate, $\Psi(t, r) = e^{-i\omega t} R(r)$, we use the Frobenius method [37]. Namely, we express the function R , written with respect to the compact coordinate x , as a product of the factor, which diverges at the singular points $x = 0$ and $x = 1$ satisfying the quasinormal boundary conditions, and the Frobenius series expansion

$$R(x) = x^{-i\omega/2\kappa_g} e^{i\omega r} r^\lambda \sum_{m=0}^{\infty} c_m x^m, \quad (8)$$

where $\kappa_g > 0$ and λ are determined by substituting the series into (7) and expanding, respectively, at $x = 0$ and $x = 1$. By expanding the wavelike equation at $x = 0$, we find the recurrence relation for the coefficients c_m , which can be numerically reduced to the three-terms relation via Gaussian eliminations. Finally, we obtain an equation with the infinite continued fraction with respect to ω . In order to calculate the infinite continued fraction we use the Nollert improvement [38], which was generalized in [39] for an arbitrary number of terms in the recurrence relation (see Sec. 3.4 of [40]). When the singular points of the wavelike equation appear within the unit circle $|x| < 1$, we employ a sequence of positive real midpoints as described in [41].

C. Gravitational perturbations of rotating black holes

The general parametrization of spherically symmetric black holes [31] was extended to the axially-symmetric case in [42]. Here, for illustration, we will consider the near-horizon deformations of the Kerr metric which fall into a particular, more symmetric class of this general parametrization. The parametrized metric includes deformations in the radial and axial directions and has the general form given by eqs. (1, 22, 67) of [43].

The wave-like equation has the form [44],

$$\Delta(r)^s(r) \frac{d}{dr} \left(\Delta(r)^{1-s} \frac{dR}{dr} \right) + \left(\frac{K^2(r) - isK(r)\Delta'(r)}{\Delta(r)} + 4is\omega r - \lambda \right) R(r) = 0, \quad (9)$$

where

$$\begin{aligned} \Delta(r) &\equiv (r^2 A(1 - r_0/r) + a^2)(1 - r_0/r), \\ K(r) &\equiv (r^2 + a^2)\omega - am, \end{aligned}$$

and λ is the separation constant. Here for the gravitational perturbations we take $s = -2$. Then we consider ad hoc deformation of the wave-like equation for gravitational perturbations of Kerr black hole via deformations implemented in $A(x)$ (4).

III. HOW TO PREPARE DEFORMATIONS SOLELY IN THE NEAR-HORIZON ZONE

A. Deformation of the black hole

In this paper we will study the nonmoderate Schwarzschild-like black holes, which have the Schwarzschild size-to-mass ratio and satisfy the post-Newtonian constraints $\epsilon = a_0 = b_0$. This choice implies that the black-hole geometry is almost Schwarzschildian everywhere starting from some distance from the black hole, which includes not only the asymptotic post-Newtonian region, but also the region around the maximum of the wave equation effective potential, photon sphere and the innermost stable circular orbit, that is, the region responsible for the dominant characteristics of various astrophysical radiation phenomena. The near-horizon geometry of such nonmoderate black holes differs significantly from the Schwarzschild ones: for instance, the nonmoderate black hole can have different Hawking temperature and/or large values of higher derivatives of the metric function, corresponding to large values of the near-horizon coefficients a_1, a_2, \dots and b_1, b_2, \dots . Overall, here we will compare the Schwarzschild black hole with the following four cases:

1. Nonmoderate Schwarzschild-like black hole with the Schwarzschild values of the Hawking temperature and radius of the event horizon (black hole 1).
2. Nonmoderate Schwarzschild-like black hole with considerably different (from the Schwarzschild one) Hawking temperature, but the same radius of the event horizon (black hole 2).
3. Moderate black hole with a slightly different radius, but the same mass and post-Newtonian behavior (black hole 3).

Thus, we study the moderate and nonmoderate near-horizon deformations of the Schwarzschild geometry.

B. Deformations of the wave-equation

In addition to the deformations of the wavelike equation due to deviation of the black-hole geometry from the General Relativity solution (Schwarzschild or Kerr geometry), we will consider the deformations due to some external (with respect to the black hole) source. These sources can lead to deformations in the near-horizon region (e.g., due to the strong-field quantum effects) or at a distance (e.g., due to accreting matter). The second situation is the most interesting, because quantum corrections in the near horizon zone in the form of bath of quantum matter fields under supposition of purely Einsteinian gravity would have incremental influence upon the metric, being localized in the tiny layer of order of

Planck length and with negligible energy density. This physically non-motivated configuration was considered in [45]. Here, we have in mind quantum corrections which, first of all, would modify the gravitational sector. Thus, we either mean astrophysical environment at a distance from the black hole or modification of gravitational sector in the near-horizon zone.

We shall consider the simplest kind of the above deformations by adding an augmentation to the effective potential in a form of a (smaller) peak,

$$V \mapsto V + \delta V, \quad (10)$$

where

$$\delta V = \frac{\delta}{r_0^2} \cosh^{-2} \frac{r_* - r_p}{r_s}, \quad (11)$$

where δ , r_p , and r_s are constants, defining, respectively, size, position, and wideness of the augmentation.

The Pöschl-Teller-like augmentation (11) not only add a localized deformation in the vicinity of $r_* = r_p$, but also changes the singular point of the wavelike differential equation (7), which corresponds to the event horizon $r = r_0$ ($r_* = -\infty$). This is because the hyperbolic cosine has irregular singular point at $r_* = \infty$. That is why, in order to model the deformation which does not affect the horizon, we consider another augmentation in the form of a rational function of r , which approaches zero at the horizon as $\delta V \propto (r - r_0)^h$ and at infinity as $\delta V \propto r^{-a}$, having the maximum value $\delta V_{max} = \delta/r_0^2$ at $r = r_m > r_0$,

$$\delta V = \frac{\delta}{r_0^2} \left(\frac{1 - r_0/r}{1 - r_0/r_m} \right)^h \left(1 + \frac{h}{a} \times \frac{r/r_m - 1}{r_m/r_0 - 1} \right)^{-a}. \quad (12)$$

IV. OVERTONES' OUTBURST

In table I we compare accurate values of seven dominant modes of the Schwarzschild black hole and three modified black holes: two nonmoderate black holes of the same size and mass (black holes 1 and 2), which are characterized by large values of the coefficient a_2 , while the coefficient a_1 can be small (then the Hawking temperature is close to the Schwarzschild one) or large (when the Hawking temperature differs a lot). At the same time, by requiring the parameter a_2 to be large, the effective potential will acquire deformation near the event horizon, but remain almost the same at a distance from the black hole. In both cases the real part of the higher overtones differ significantly from the Schwarzschild spectrum. It is essential that the latter case corresponds to a very small deformation of the effective potential (fig. 1), so that even tiny deformations near the event horizon are sufficient for the outburst of overtones. When a_1 is not small, the difference is larger, and the spacing of the imaginary part also differs considerably, leading to quite a large difference already in the second overtone. The fundamental

Schwarzschild	black hole 1	D_{Re}	D_{Im}	black hole 2	D_{Re}	D_{Im}	black hole 3	D
$s = 0, \ell = 1$								
0.585872 - 0.195320i	0.587258 - 0.197245i	0.24%	0.99%	0.587765 - 0.193327i	0.32%	1.02%	0.583061 - 0.195929i	0.466%
0.528897 - 0.612515i	0.526080 - 0.617827i	0.53%	0.87%	0.561322 - 0.568479i	6.13%	7.19%	0.524958 - 0.614911i	0.570%
0.459079 - 1.080267i	0.447096 - 1.087917i	2.61%	0.71%	0.679860 - 0.931860i	48.1%	13.7%	0.453920 - 1.085471i	0.624%
0.406517 - 1.576596i	0.379277 - 1.585328i	6.70%	0.55%	0.898879 - 1.342045i	121%	14.9%	0.400556 - 1.584962i	0.631%
0.370218 - 2.081524i	0.319572 - 2.090056i	13.7%	0.41%	1.144760 - 1.754668i	209%	15.7%	0.363661 - 2.093076i	0.628%
0.344154 - 2.588239i	0.256746 - 2.595787i	25.4%	0.29%	1.404472 - 2.162571i	308%	16.4%	0.337075 - 2.602974i	0.626%
0.324452 - 3.094880i	0.164957 - 3.102742i	49.2%	0.25%	1.671835 - 2.566564i	415%	17.1%	0.316883 - 3.112805i	0.625%
$s = 1, \ell = 1$								
0.496527 - 0.184975i	0.497286 - 0.186510i	0.15%	0.83%	0.499888 - 0.184026i	0.68%	0.51%	0.493495 - 0.185416i	0.578%
0.429031 - 0.587335i	0.425875 - 0.591467i	0.74%	0.70%	0.477337 - 0.570306i	11.3%	2.90%	0.424652 - 0.589368i	0.664%
0.349547 - 1.050375i	0.337877 - 1.056161i	3.34%	0.55%	0.579548 - 0.976294i	65.8%	7.05%	0.343812 - 1.055308i	0.683%
0.292353 - 1.543818i	0.267031 - 1.550075i	8.66%	0.41%	0.783696 - 1.404047i	168%	9.05%	0.285850 - 1.552058i	0.668%
0.253108 - 2.045101i	0.208316 - 2.050006i	17.7%	0.24%	1.019914 - 1.827973i	302%	10.6%	0.246129 - 2.056707i	0.657%
0.224506 - 2.547851i	0.153282 - 2.548313i	31.7%	0.02%	1.270965 - 2.244820i	466%	11.9%	0.217204 - 2.562872i	0.653%
0.202429 - 3.050533i	0.096081 - 3.040733i	52.5%	0.32%	1.530215 - 2.656275i	656%	12.9%	0.194916 - 3.069024i	0.653%
$s = 0, \ell = 2$								
0.967288 - 0.193518i	0.970301 - 0.195678i	0.31%	1.12%	0.968930 - 0.193534i	0.17%	0.01%	0.962830 - 0.194098i	0.456%
0.927701 - 0.591208i	0.927929 - 0.597500i	0.03%	1.06%	0.890084 - 0.593171i	4.06%	0.33%	0.922453 - 0.593168i	0.509%
0.861088 - 1.017117i	0.855454 - 1.027058i	0.65%	0.98%	0.895286 - 0.760648i	3.97%	25.2%	0.854530 - 1.021068i	0.575%
0.787726 - 1.476193i	0.772643 - 1.489215i	1.91%	0.88%	1.115236 - 1.148286i	41.6%	22.2%	0.779838 - 1.482817i	0.616%
0.722598 - 1.959843i	0.693764 - 1.975524i	3.99%	0.80%	1.320778 - 1.558055i	82.8%	20.5%	0.713655 - 1.969520i	0.631%
0.669799 - 2.456822i	0.621746 - 2.475224i	7.17%	0.75%	1.550726 - 1.970153i	131%	19.8%	0.660043 - 2.469663i	0.633%
0.627772 - 2.959909i	0.552750 - 2.982487i	12.0%	0.76%	1.796557 - 2.380874i	186%	19.6%	0.617342 - 2.975931i	0.632%
$s = 1, \ell = 2$								
0.915191 - 0.190009i	0.917791 - 0.192048i	0.28%	1.07%	0.916726 - 0.189735i	0.16%	0.14%	0.910635 - 0.190547i	0.491%
0.873085 - 0.581420i	0.872888 - 0.587320i	0.02%	1.02%	0.847080 - 0.565277i	2.98%	2.78%	0.867671 - 0.583268i	0.545%
0.802373 - 1.003175i	0.796272 - 1.012369i	0.76%	0.92%	0.866621 - 0.795077i	8.01%	20.7%	0.795527 - 1.006997i	0.610%
0.725190 - 1.460397i	0.709557 - 1.472175i	2.16%	0.81%	1.060272 - 1.178507i	46.2%	19.3%	0.716892 - 1.466942i	0.648%
0.657473 - 1.943219i	0.628022 - 1.956894i	4.48%	0.70%	1.261355 - 1.595636i	91.8%	17.9%	0.648021 - 1.952893i	0.659%
0.602986 - 2.439430i	0.554449 - 2.454492i	8.05%	0.62%	1.487023 - 2.014416i	146%	17.4%	0.592630 - 2.452356i	0.659%
0.559690 - 2.941586i	0.485002 - 2.958068i	13.3%	0.56%	1.728792 - 2.430765i	208%	17.4%	0.548569 - 2.957790i	0.656%

TABLE I. The dominant mode and first six overtones calculated using the Frobenius method in the units $r_0 = 2M = 1$ ($\epsilon = 0$) for the Schwarzschild black hole ($a_1 = b_1 = 0$, $T_H^{(0)} = 1/4\pi$), the black hole 1: $a_1 = 0.0001$, $a_2 = -1000$, $a_3 = 1001$, $a_4 = 0$, $b_1 = 0$ ($T_H = 1.0001T_H^{(0)}$), the black hole 2: $a_1 = 0.5$, $a_2 = 100$, $a_3 = 0$, $b_1 = 0$ ($T_H = 1.5T_H^{(0)}$), and the black hole 3 with $\epsilon = -0.01$ ($2M = 1$, $a_1 = b_1 = 0$), and the relative differences (in per cents) of the corresponding modes from the Schwarzschild ones.

mode and overtones of the moderate black hole 3 change softly, not showing high sensitivity of overtones relatively the lowest mode. There remains the other (a trivial in a sense) case which we did not consider: if the asymptotic parameter ϵ differs a lot from zero, which leads to large deviations of both the fundamental mode and overtones from their Schwarzschild values.

From the data presented in table I, we can see that the black hole whose Hawking temperature differs by 1.5 times from the Schwarzschild's one, the effect of the deviation of overtones is strong already at $n = 2$ case. As pointed out in [45], the second overtone of the black hole 2 for $\ell = 2$ was missed in the first version of our paper.

This mode has almost the same real part as $n = 1$ while imaginary part is significantly differs both from $n = 1$ and $n = 2$ Schwarzschild modes. This case shows that not only the real part of ω , but also the damping rate may experience an outburst.

In table II one can see that the same high sensitivity of overtones takes place for the near-horizon deformations of the equation for the gravitational perturbations of rotating black holes.

The pronounced sensitivity of overtone frequencies to small near-horizon deformations is not the only reason to study overtones. Another important aspect is the excitation factors of the overtones, which, as shown in particu-

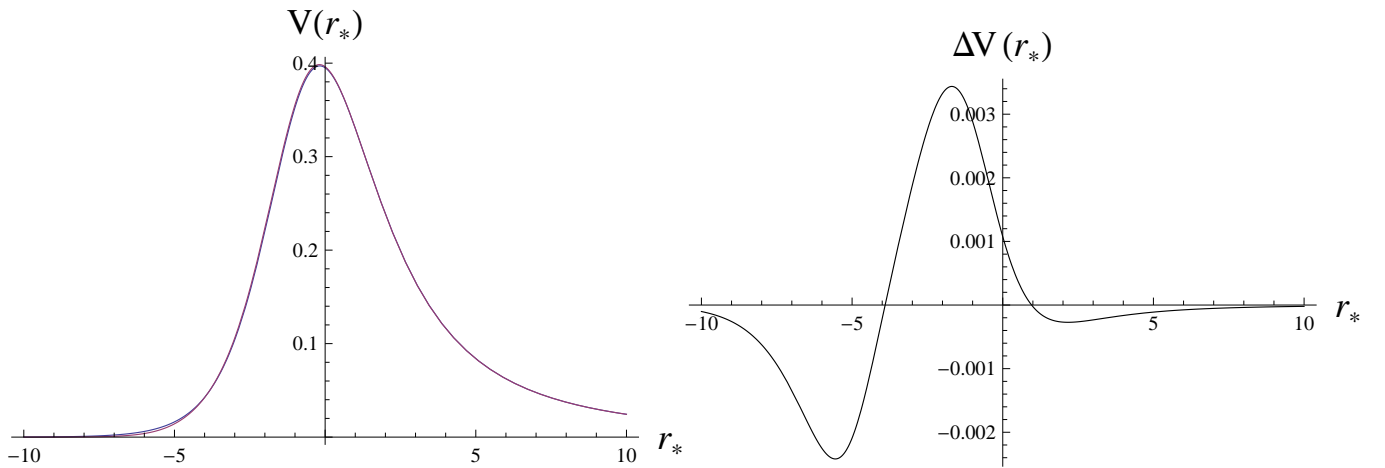


FIG. 1. Left panel: Effective potentials ($s = 0$, $\ell = 1$, $r_0 = 2M = 1$) for the black hole 2 (blue) and Schwarzschild black hole (red) for comparison. Right panel: difference between the potentials.

n	Kerr	modified Kerr	D_{Re}	D_{Im}
0	$0.586017 - 0.075630i$	$0.590393 - 0.075233i$	0.75%	0.52%
1	$0.577922 - 0.228149i$	$0.578766 - 0.226295i$	0.15%	0.81%
2	$0.562240 - 0.383895i$	$0.548651 - 0.391231i$	2.42%	1.91%
3	$0.538956 - 0.542888i$	$0.488262 - 0.616589i$	9.41%	13.6%
4	$0.506263 - 0.697962i$	$0.597420 - 0.814367i$	18.0%	16.7%
5	$0.486283 - 0.830803i$	$0.709014 - 0.975480i$	45.8%	17.4%
6	$0.499165 - 0.983084i$	$0.829156 - 1.138613i$	66.1%	15.8%
7	$0.506652 - 1.156708i$	$0.951035 - 1.299293i$	87.7%	12.3%

TABLE II. Dominant modes of gravitational perturbations ($\ell = m = 2$) for the Kerr black hole $a = 0.8$, $M = 1$, $r_0 = 1.6$ ($\epsilon = 0.25$) calculated in [46] compared to the modified Kerr ($a_1 = 0.5$, $a_2 = 100$, $a_3 = 0$) and their relative differences (in per cents).

lar examples in [47], may also increase significantly. Although the energy content of overtones is generally much smaller than that carried by the fundamental mode, this leads to a weaker observational prospect for overtones.

Now, suppose there is some form of deformation near the event horizon due to new physics. This leads to two effects: a modification of the signal in the early ring-down phase and a modification of the signal at very late times, when the signal is strongly damped. The latter effect is known as echoes [5] and has been widely studied in recent literature. In this paper, we will demonstrate that the energy carried by overtones is much greater than that of echoes. Therefore, overtones offer a much more promising observational aspect of black hole spectra compared to echoes.

On fig. 2 we show the illustration of the same principle via the near-horizon deformation of the effective potential for gravitational perturbations of the Schwarzschild black hole by a Pöschl-Teller-like augmentation. The time-domain integration gives similar ringdown profiles

for Schwarzschild and deformed potentials, but after the deduction of the fundamental-mode contribution via the Prony method one can see that the amplitude of the first overtone is many orders larger than the echoes produced at late times due to reflection from the Pöschl-Teller-like peak near the event horizon. Thus, the first overtone may be more perspective for probing the event horizon than the still elusive echoes. Another observational perspective of the overtones' outburst is related to the highly probable breakdown of isospectrality in a modified theory of gravity, like it happens for example in the Einstein-dilaton-Gauss-Bonnet and a number of other theories. In [29] it was shown that because of the disentanglement between axial and polar GW parities, the overtones outburst may already occur within the near-future detection range.

V. DISTINGUISHING NEAR HORIZON DEFORMATIONS FROM ASTROPHYSICAL ENVIRONMENT

An important question remains whether it is possible that a tiny perturbation of the effective potential in the far zone, owing to black holes environment, such as an accretion disk, also produces the outburst of overtones [28, 29]? If so, then it would be difficult to distinguish the latter from the near-horizon deformations. For this purpose as an example we consider a simple augmentation of the Schwarzschild potential in the form given by Eq. (12).

We take $\delta = 0.006$, which is two orders smaller than the height of the main Schwarzschild peak for $\ell = 2$ (see Fig. 3). Note, that the maximum deformation is of the same order as the one considered in Table I of [29]. Having in mind various types of possible astrophysical environment, choosing the value of $\delta \sim 10^{-3}$ is excessively big. For example, the Shakura-Sunyaev disk model typ-

n	Schwarzschild	$\delta = 0.0006, r_m = 20r_0$	$\delta = 0.006, r_m = 20r_0$	$\delta = 0.006, r_m = 50r_0$
0	0.747343 – 0.177925 <i>i</i>	0.747345 – 0.177928 <i>i</i>	0.747360 – 0.177957 <i>i</i>	0.747351 – 0.177937 <i>i</i>
1	0.693422 – 0.547830 <i>i</i>	0.693457 – 0.547810 <i>i</i>	0.693776 – 0.547640 <i>i</i>	0.693555 – 0.547738 <i>i</i>
2	0.602107 – 0.956554 <i>i</i>	0.602036 – 0.956371 <i>i</i>	0.601425 – 0.954672 <i>i</i>	0.601761 – 0.955865 <i>i</i>
3	0.503010 – 1.410296 <i>i</i>	0.502438 – 1.410320 <i>i</i>	0.496956 – 1.410590 <i>i</i>	0.500803 – 1.410580 <i>i</i>
4	0.415029 – 1.893690 <i>i</i>	0.414407 – 1.894740 <i>i</i>	0.409708 – 1.905080 <i>i</i>	0.413087 – 1.897930 <i>i</i>
5	0.338599 – 2.391216 <i>i</i>	0.339163 – 2.393330 <i>i</i>	0.346480 – 2.409976 <i>i</i>	0.341543 – 2.398760 <i>i</i>

TABLE III. Dominant modes of axial gravitational perturbations for the Schwarzschild black hole ($\ell = 2$) compared with the ones for the potential deformed by augmentation (12) with $h = a = 15$: the second column corresponds to the maximum deformation of the order of 0.1% of the Schwarzschild potential peak and the last two columns correspond to higher deformation of the order of 1% placed at different distances from the black hole. The modes are calculated using the Frobenius method in the units $r_0 = 2M = 1$.

ically assumes that density of the accreting matter for the stellar-mass black holes, $\rho \leq 100g/cm^3$ (see [48, 49] for review), which is more than 10 orders of magnitude smaller than the black-hole “density”. For larger black holes the effects due to accreting matter are even smaller. We have considered such big value of δ not only as a stress test for distinguishing the environmental effects, but also not to resort to time consuming computations of tiny changing of the frequencies.

Such astrophysically big deformation of the potential leads to very small corrections of the first several overtones (see table III) and the corrections become even smaller if we shift the deformation farther from the black hole. Unlike the deformation considered in [28, 29], the deformation (12) by construction does not affect the near-horizon behavior of the effective potential. Therefore we conclude that the phenomenon of the overtone outburst indeed happens due to deformations near the horizon.

If one takes sufficiently large values of δ , providing the bump’s height of the same order as the main peak, the overtones certainly become much more sensitive to such a modification, e.g., for $\delta = 0.1$ the real part of the higher overtones can be several times smaller than the Schwarzschild value. However, such a modification of the effective potential cannot be considered as a small deformation due to environment and is obviously physically irrelevant. These results are in agreement with the previous works: In [30] it was shown that for small bumps in the far zone, no outburst of overtones are observed, while in [50] the stability of the fundamental mode was found even for relatively large bumps.

VI. CONCLUSIONS

We have shown that a small deformation of the near-horizon geometry of a black hole leads to a very strong change of overtones, while the fundamental mode remains almost unchanged. It immediately follows that first few overtones can probe the event horizon geometry which potentially could be seen at the earlier stage of quasinor-

mal ringing [9].

The observed here phenomenon of high sensitivity of lowest overtones to small deformations of the near horizon geometry is definitely connected with the so called “overtones instability” discussed in [28, 29]. There the effective potential was deformed by a sinusoidal function, so that this would correspond to the small deformation of the geometry not only near the event horizon, but in the whole space. Moreover, in [28, 29] the derivative of the deformation function does not vanish at the event horizon, implying nonsmall changes of the near-horizon geometry, and the impact of the deformation obviously increases when the “high-frequency” deformation is considered.

Such a setup does not allow one to understand which kind of deformations produce the outburst of overtones, which is the main question of our consideration. Here we have shown that very small deformations in a relatively small region near the event horizon are sufficient for such an outburst of overtones, while the deformations at a distance from the black hole need to be very large and physically irrelevant in order to produce a similar effect. Having a number of overtones in addition to the fundamental mode and using the strict hierarchy of coefficients of the parametrization [31, 42], one could, in principle, constrain the allowed black-hole geometry.

The high sensitivity of the overtones due to the small nonsmooth deformations, which is also the case of the random deformation probes of [28], were studied also in earlier works [51–53]. The crucial difference between our approach and the above works is that we considered smooth deformations distributed over some region near the horizon (when considering the horizon contribution, see Figs. 1, 2) and in the far zone (when considering the astrophysical environment, Eq. 12). This must be more appropriate to real astrophysical distribution of gravitational and matter fields than the nonlocalized deformations of [28, 29] or nonsmooth highly localised (“ultraviolet”) deformations considered in [28, 51–53]. After all, the latter high-frequency deformations of the black-hole spacetime would require high energies which could hardly

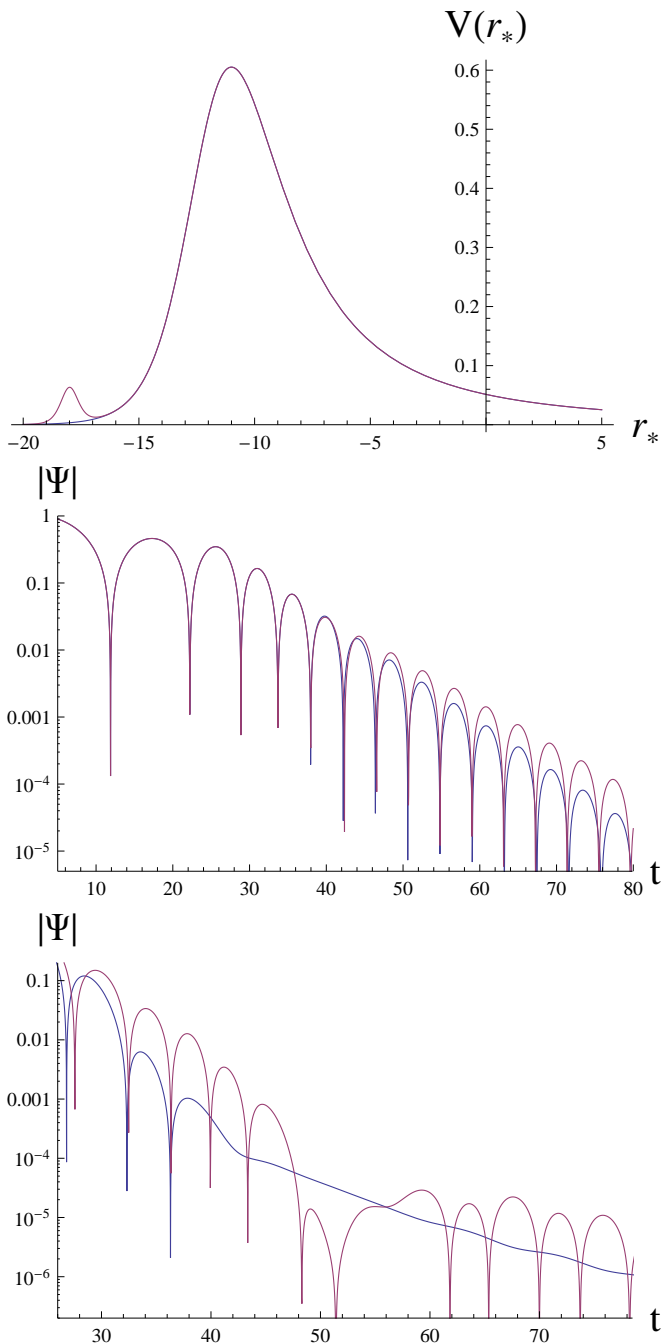


FIG. 2. Upper panel: The effective potential at $r_* = 0$ corresponding to $r = 10$ for the $\ell = 2$ axial gravitational perturbations of the Schwarzschild ($r_0 = 2M = 1$) black hole (blue) and the potential deformed by a Pöschl-Teller-like augmentation $\delta V = 0.06/\cosh^2(2r_* + 36)$ (red). Middle panel: the corresponding time-domain profiles. Lower panel: the time-domain profiles without the dominant-mode contribution, calculated with the Prony method, $\omega_0 \approx 0.7473 - 0.1779i$ for the Schwarzschild black hole and $\omega_0 \approx 0.7622 - 0.1491i$ for the deformed potential. The amplitude, corresponding to the first overtone, is about four orders larger than the amplitude of the echo, appearing at $t \simeq 60$ (red). For an illustration, the augmentation is chosen to be large in order to compare the overtones effect with the echoes at earlier times.

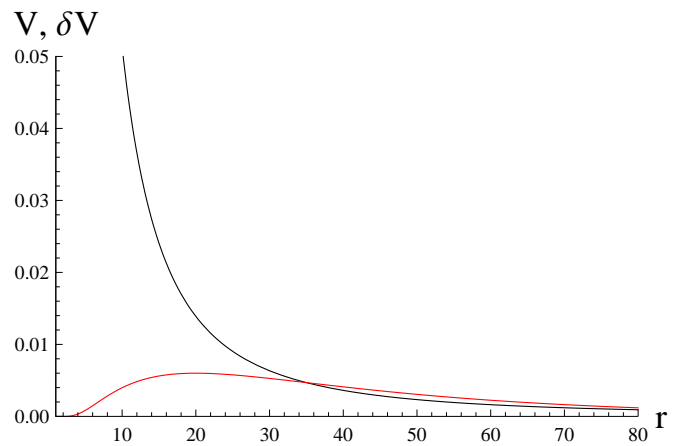


FIG. 3. The effective potential for the $\ell = 2$ gravitational perturbations of the Schwarzschild black hole (black) and the augmentation, defined by Eq. 12 for $\delta = 0.006$, $r_m = 20$, $h = a = 15$. The numerical values of the quasinormal modes are given in table III.

be ascribed to an astrophysical environment in the linear regime.

It's also crucial to recognize that the influence of the near-horizon geometry, reflecting in the initial overtones, isn't restricted solely to minor deviations from the Schwarzschild/Kerr geometries in the near-horizon region. This is because strong constraints on the near-horizon geometry of black holes remain elusive. Since the initial version of this work was published on arXiv, several specific instances highlighting the sensitivity of overtones have been examined. An outburst of overtones is expected for virtually any metric that is modified in the near-horizon zone. The only difference lies in the rate at which the deviation occurs, meaning the overtone number at which the deviation becomes significant. From a practical perspective, if such a strong deviation does not appear within the first few overtones, it will not have any potential for observational relevance. Black hole metrics in various alternative theories of gravity often differ significantly in the near-horizon zone, indicating a promising future direction for studying overtones within alternative gravity theories.

In cases where deformations were significant in the near-horizon area but minor or moderate in the radiation zone, notable behaviors, even in the first and second overtones, were observed. Thus, for the Hayward, Bonanno-Reuter, and Schwarzschild-AdS black holes the qualitatively new behavior occurs already at $n = 1$ where a purely imaginary modes may appear, while higher n differ from their Schwarzschild values by tens and, sometimes, more than 100% percents. We can consolidate these specific instances across various alternative theories of gravity in Table IV. However, the majority of the aforementioned works, while capturing the qualitative behavior of the overtone outburst, focus on perturbations of test fields. Thus, this program is in the very beginning,

Metric	n	publication
Hayward	1	[27, 54]
Bonnano-Reuter	1	[27]
Dymnikova	3	[55]
Bardeen	4	[56, 57]
Einstein-Weyl	4	[58]
D-dimensional Einstein-(GB)-AdS	1	[59]
sub-Planckian curvature	4	[60]
effective quantum gravity	2	[61]
quantum Oppenheimer-Snyder model	2	[62]

TABLE IV. Outburst of overtones for various theories of gravity and the minimal number of n which shows distinctive behavior.

because no thorough investigation of overtones' behavior for gravitational perturbations have been made in alter-

native theories of gravity.

Note that, while overtones are not the only theoretical method for probing near-horizon geometry, they may be one of the most promising approaches. This is because echoes correspond to a much weaker signal, while the black hole shadow primarily provides information about the geometry of the photon sphere. However, in the case of near-extremal rotating black holes, the photon sphere approaches the event horizon. In this regime, the shadows cast by black holes, as well as the fundamental mode, may indeed reveal information about the near-horizon geometry [63, 64].

ACKNOWLEDGMENTS

A. Z. was supported by Conselho Nacional de Desenvolvimento Científico e Tecnológico (CNPq).

-
- [1] Hans-Peter Nollert. TOPICAL REVIEW: Quasinormal modes: the characteristic ‘sound’ of black holes and neutron stars. *Class. Quant. Grav.*, 16:R159–R216, 1999.
- [2] Kostas D. Kokkotas and Bernd G. Schmidt. Quasinormal modes of stars and black holes. *Living Rev. Rel.*, 2:2, 1999.
- [3] Emanuele Berti, Vitor Cardoso, and Andrei O. Starinets. Quasinormal modes of black holes and black branes. *Class. Quant. Grav.*, 26:163001, 2009.
- [4] R. A. Konoplya and A. Zhidenko. Quasinormal modes of black holes: From astrophysics to string theory. *Rev. Mod. Phys.*, 83:793–836, 2011.
- [5] Vitor Cardoso, Edgardo Franzin, and Paolo Pani. Is the gravitational-wave ringdown a probe of the event horizon? *Phys. Rev. Lett.*, 116(17):171101, 2016. [Erratum: *Phys.Rev.Lett.* 117, 089902 (2016)].
- [6] Thibault Damour and Sergey N. Solodukhin. Wormholes as black hole foils. *Phys. Rev. D*, 76:024016, 2007.
- [7] R. A. Konoplya and A. Zhidenko. Wormholes versus black holes: quasinormal ringing at early and late times. *JCAP*, 12:043, 2016.
- [8] Sumanta Chakraborty, Elisa Maggio, Anupam Mazumdar, and Paolo Pani. Implications of the quantum nature of the black hole horizon on the gravitational-wave ringdown. *Phys. Rev. D*, 106(2):024041, 2022.
- [9] Matthew Giesler, Maximiliano Isi, Mark A. Scheel, and Saul Teukolsky. Black Hole Ringdown: The Importance of Overtones. *Phys. Rev. X*, 9(4):041060, 2019.
- [10] Naritaka Oshita. Ease of excitation of black hole ringing: Quantifying the importance of overtones by the excitation factors. *Phys. Rev. D*, 104(12):124032, 2021.
- [11] Xisco Jiménez Forteza and Pierre Mourier. High-overtone fits to numerical relativity ringdowns: Beyond the dismissed $n=8$ special tone. *Phys. Rev. D*, 104(12):124072, 2021.
- [12] Naritaka Oshita. Thermal ringdown of a Kerr black hole: overtone excitation, Fermi-Dirac statistics and greybody factor. *JCAP*, 04:013, 2023.
- [13] Maximiliano Isi, Matthew Giesler, Will M. Farr, Mark A. Scheel, and Saul A. Teukolsky. Testing the no-hair theorem with GW150914. *Phys. Rev. Lett.*, 123(11):111102, 2019.
- [14] B. P. Abbott et al. Binary Black Hole Mergers in the first Advanced LIGO Observing Run. *Phys. Rev. X*, 6(4):041015, 2016. [Erratum: *Phys.Rev.X* 8, 039903 (2018)].
- [15] Maximiliano Isi and Will M. Farr. Analyzing black-hole ringdowns. *arXiv:2107.05609*, 7 2021.
- [16] Marco Crisostomi, Kallol Dey, Enrico Barausse, and Roberto Trotta. Neural posterior estimation with guaranteed exact coverage: The ringdown of GW150914. *Phys. Rev. D*, 108(4):044029, 2023.
- [17] M. Punturo et al. The Einstein Telescope: A third-generation gravitational wave observatory. *Class. Quant. Grav.*, 27:194002, 2010.
- [18] Sheila Dwyer, Daniel Sigg, Stefan W. Ballmer, Lisa Barsotti, Nergis Mavalvala, and Matthew Evans. Gravitational wave detector with cosmological reach. *Phys. Rev. D*, 91(8):082001, 2015.
- [19] Pau Amaro-Seoane et al. Laser Interferometer Space Antenna. *arXiv:1702.00786*, 2 2017.
- [20] Collin D. Capano, Miriam Cabero, Julian Westerweck, Jahed Abedi, Shilpa Kastha, Alexander H. Nitz, Yi-Fan Wang, Alex B. Nielsen, and Badri Krishnan. Multimode Quasinormal Spectrum from a Perturbed Black Hole. *Phys. Rev. Lett.*, 131(22):221402, 2023.
- [21] Roberto Cotesta, Gregorio Carullo, Emanuele Berti, and Vitor Cardoso. Analysis of Ringdown Overtones in GW150914. *Phys. Rev. Lett.*, 129(11):111102, 2022.
- [22] Laura Sberna, Pablo Bosch, William E. East, Stephen R. Green, and Luis Lehner. Nonlinear effects in the black hole ringdown: Absorption-induced mode excitation. *Phys. Rev. D*, 105(6):064046, 2022.
- [23] Mark Ho-Yeuk Cheung et al. Nonlinear Effects in Black Hole Ringdown. *Phys. Rev. Lett.*, 130(8):081401, 2023.
- [24] Keefe Mitman et al. Nonlinearities in Black Hole Ringdowns. *Phys. Rev. Lett.*, 130(8):081402, 2023.

- [25] Naritaka Oshita and Daichi Tsuna. Slowly decaying ring-down of a rapidly spinning black hole: Probing the no-hair theorem by small mass-ratio mergers with LISA. *Phys. Rev. D*, 108(10):104031, 2023.
- [26] Prashant Kocherlakota et al. Constraints on black-hole charges with the 2017 EHT observations of M87*. *Phys. Rev. D*, 103(10):104047, 2021.
- [27] R. A. Konoplya, A. F. Zinhailo, J. Kunz, Z. Stuchlik, and A. Zhidenko. Quasinormal ringing of regular black holes in asymptotically safe gravity: the importance of overtones. *JCAP*, 10:091, 2022.
- [28] José Luis Jaramillo, Rodrigo Panosso Macedo, and Lamis Al Sheikh. Pseudospectrum and Black Hole Quasinormal Mode Instability. *Phys. Rev. X*, 11(3):031003, 2021.
- [29] José Luis Jaramillo, Rodrigo Panosso Macedo, and Lamis Al Sheikh. Gravitational Wave Signatures of Black Hole Quasinormal Mode Instability. *Phys. Rev. Lett.*, 128(21):211102, 2022.
- [30] Mark Ho-Yeuk Cheung, Kyriakos Destounis, Rodrigo Panosso Macedo, Emanuele Berti, and Vitor Cardoso. Destabilizing the Fundamental Mode of Black Holes: The Elephant and the Flea. *Phys. Rev. Lett.*, 128(11):111103, 2022.
- [31] Luciano Rezzolla and Alexander Zhidenko. New parametrization for spherically symmetric black holes in metric theories of gravity. *Phys. Rev. D*, 90(8):084009, 2014.
- [32] R. A. Konoplya, J. Kunz, and A. Zhidenko. Blandford-Znajek mechanism in the general stationary axially-symmetric black-hole spacetime. *JCAP*, 12(12):002, 2021.
- [33] R. A. Konoplya and A. Zhidenko. General parametrization of black holes: The only parameters that matter. *Phys. Rev. D*, 101(12):124004, 2020.
- [34] R. A. Konoplya and A. Zhidenko. Shadows of parametrized axially symmetric black holes allowing for separation of variables. *Phys. Rev. D*, 103(10):104033, 2021.
- [35] Carsten Gundlach, Richard H. Price, and Jorge Pullin. Late time behavior of stellar collapse and explosions: 1. Linearized perturbations. *Phys. Rev. D*, 49:883–889, 1994.
- [36] J.F. Hauer, C.J. Demeure, and L.L. Scharf. Initial results in Prony analysis of power system response signals. *IEEE Transactions on Power Systems.*, 5:80–89, 1990.
- [37] E. W. Leaver. An Analytic representation for the quasi normal modes of Kerr black holes. *Proc. Roy. Soc. Lond. A*, 402:285–298, 1985.
- [38] Hans-Peter Nollert. Quasinormal modes of Schwarzschild black holes: The determination of quasinormal frequencies with very large imaginary parts. *Phys. Rev. D*, 47:5253–5258, 1993.
- [39] Alexander Zhidenko. Massive scalar field quasi-normal modes of higher dimensional black holes. *Phys. Rev. D*, 74:064017, 2006.
- [40] Alexander Zhidenko. *Linear perturbations of black holes: stability, quasi-normal modes and tails*. PhD thesis, Sao Paulo U., 2009.
- [41] Andrzej Rostworowski. Quasinormal frequencies of D-dimensional Schwarzschild black holes: Evaluation via continued fraction method. *Acta Phys. Polon. B*, 38:81–89, 2007.
- [42] Roman Konoplya, Luciano Rezzolla, and Alexander Zhidenko. General parametrization of axisymmetric black holes in metric theories of gravity. *Phys. Rev. D*, 93(6):064015, 2016.
- [43] R. A. Konoplya, Z. Stuchlik, and A. Zhidenko. Axisymmetric black holes allowing for separation of variables in the Klein-Gordon and Hamilton-Jacobi equations. *Phys. Rev. D*, 97(8):084044, 2018.
- [44] P. Kanti, R. A. Konoplya, and A. Zhidenko. Quasi-Normal Modes of Brane-Localised Standard Model Fields. II. Kerr Black Holes. *Phys. Rev. D*, 74:064008, 2006.
- [45] Vitor Cardoso, Shilpa Kastha, and Rodrigo Panosso Macedo. On the physical significance of black hole quasinormal mode spectra instability. *arXiv:2404.01374*, 4 2024.
- [46] Emanuele Berti, Vitor Cardoso, and Clifford M. Will. On gravitational-wave spectroscopy of massive black holes with the space interferometer LISA. *Phys. Rev. D*, 73:064030, 2006.
- [47] Hector O. Silva, Giovanni Tambalo, Kostas Glampedakis, Kent Yagi, and Jan Steinhoff. Quasinormal modes and their excitation beyond general relativity. *Phys. Rev. D*, 110(2):024042, 2024.
- [48] Marek A. Abramowicz and P. Chris Fragile. Foundations of Black Hole Accretion Disk Theory. *Living Rev. Rel.*, 16:1, 2013.
- [49] Robert F. Penna, Aleksander Sądowski, and Jonathan C. McKinney. Thin-disc theory with a non-zero-torque boundary condition and comparisons with simulations: Thin-disc theory and simulations. *Monthly Notices of the Royal Astronomical Society*, 420(1):684–698, December 2011.
- [50] Emanuele Berti, Vitor Cardoso, Mark Ho-Yeuk Cheung, Francesco Di Filippo, Francisco Duque, Paul Martens, and Shinji Mukohyama. Stability of the fundamental quasinormal mode in time-domain observations against small perturbations. *Phys. Rev. D*, 106(8):084011, 2022.
- [51] M. V. Berry. Semiclassically weak reflections above analytic and non-analytic potential barriers. *J. Phys. A: Math. Gen.*, 15:3693, 1982.
- [52] Hans-Peter Nollert. About the significance of quasinormal modes of black holes. *Phys. Rev. D*, 53:4397–4402, 1996.
- [53] J. M. Aguirregabiria and C. V. Vishveshwara. Scattering by black holes: A Simulated potential approach. *Phys. Lett. A*, 210:251–254, 1996.
- [54] R. A. Konoplya. Quasinormal modes and grey-body factors of regular black holes with a scalar hair from the Effective Field Theory. *JCAP*, 07:001, 2023.
- [55] R. A. Konoplya, Z. Stuchlik, A. Zhidenko, and A. F. Zinhailo. Quasinormal modes of renormalization group improved Dymnikova regular black holes. *Phys. Rev. D*, 107(10):104050, 2023.
- [56] R. A. Konoplya, D. Ovchinnikov, and B. Ahmedov. Bardeen spacetime as a quantum corrected Schwarzschild black hole: Quasinormal modes and Hawking radiation. *Phys. Rev. D*, 108(10):104054, 2023.
- [57] S. V. Bolokhov. Long-lived quasinormal modes and oscillatory tails of the Bardeen spacetime. *Phys. Rev. D*, 109(6):064017, 2024.
- [58] R. A. Konoplya. Quasinormal modes in higher-derivative gravity: Testing the black hole parametrization and sensitivity of overtones. *Phys. Rev. D*, 107(6):064039, 2023.
- [59] R. A. Konoplya and A. Zhidenko. Overtones’ outburst of asymptotically AdS black holes. *Phys. Rev. D*,

- 109(4):043014, 2024.
- [60] Dan Zhang, Huajie Gong, Guoyang Fu, Jian-Pin Wu, and Qiyuan Pan. Quasinormal modes of a regular black hole with sub-Planckian curvature. *Eur. Phys. J. C*, 84(6):564, 2024.
- [61] R. A. Konoplya and O. S. Stashko. Probing the Effective Quantum Gravity via Quasinormal Modes and Shadows of Black Holes. *arXiv: 2408.02578*, 8 2024.
- [62] A. F. Zinhailo. Black Hole in the Quantum Oppenheimer-Snyder model: long lived modes and the overtones' behavior. *Research Gate Preprint: doi:10.13140/RG.2.2.26785.01124*, 2024.
- [63] Gary T. Horowitz, Maciej Kolanowski, Grant N. Remmen, and Jorge E. Santos. Extremal Kerr Black Holes as Amplifiers of New Physics. *Phys. Rev. Lett.*, 131(9):091402, 2023.
- [64] Kazunori Akiyama et al. First M87 Event Horizon Telescope Results. V. Physical Origin of the Asymmetric Ring. *Astrophys. J. Lett.*, 875(1):L5, 2019.